Comparison of the Magnetic Field Inferred by SO/PHI-HRT and SDO/HMI

Jonas Sinjan, D.Calchetti, J. Hirzberger, S. K. Solanki, J. C. del Toro Iniesta, J. Woch, A. Gandorfer, A. Alvarez-Herrero, T. Appourchaux, R. Volkmer, D. Orozco Suárez and SO/PHI Team

MAX PLANCK INSTITUTE FOR SOLAR SYSTEM RESEARCH

INTRODUCTION

On 7th March 2022, Solar Orbiter crossed the Sun-Earth line at 0.5 AU. This allowed the SO/PHI-HRT[1] data to be compared with data from the similar SDO/HMI[2] instrument orbiting the Earth. Performing a cross-calibration between these two is vital for stereoscopic analysis with both instruments.

As shown below in the table, the magnetic field vector (**B**) and line-of-sight (LOS) component are compared. Note that ME denotes Milne-Eddington, implying that ME-B_{LOS} is derived via a radiative transfer inversion of the Stokes parameters using the ME approximation to obtain the full magnetic field vector, while B_{LOS} is derived without a radiative transfer inversion. **B**, consists of the magnetic field strength, |**B**|, magnetic field inclination, ɣ, and magnetic field azimuth, ϕ.

HMI (Cadence)	HRT (Cadence)
B = |B|, ɣ, ϕ (720s, 90s)	B = |B|, ɣ, ϕ (60s)
ME-B_{LOS} (720s,90s)	ME-B_{LOS} (60s)
B_{LOS} (720s, 45s)	-

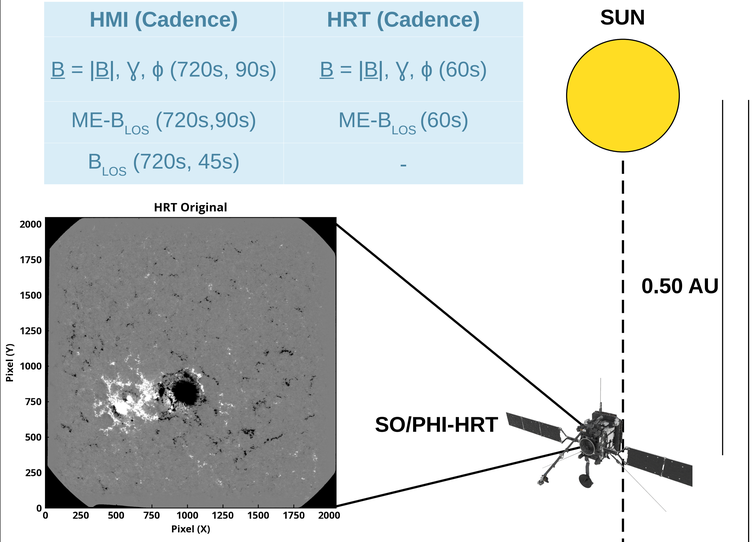

Fig. 1. Magnetogram from SO/PHI-HRT on 7 March 2022. Saturated at +/-200G.

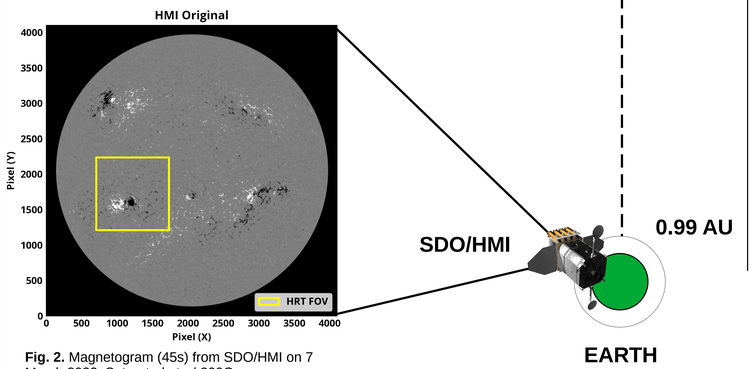

Fig. 2. Magnetogram (45s) from SDO/HMI on 7 March 2022. Saturated at +/-200G.

METHOD

1. Re-project co-temporal HMI datasets onto HRT frame[3]
2. Resample HRT datasets to match HMI spatial resolution
3. Correct residual offsets of image pairs
4. Perform a linear fit, taking into account the error in both instruments

RESULTS

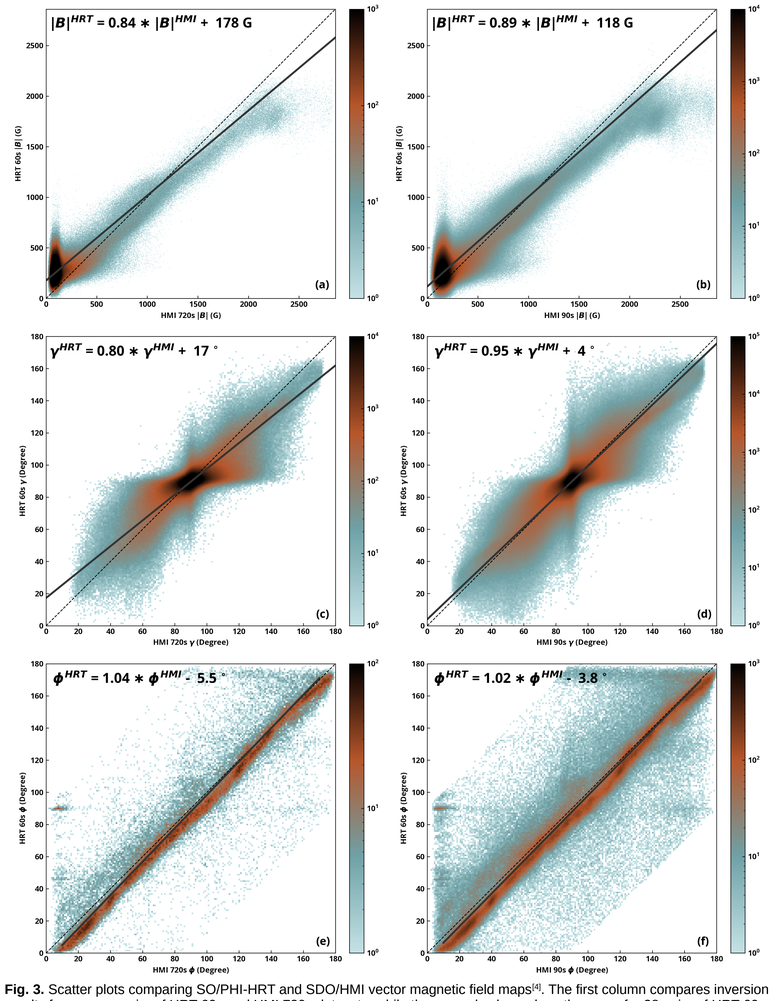

Fig. 3. Scatter plots comparing SO/PHI-HRT and SDO/HMI vector magnetic field maps[4]. The first column compares inversion results from seven pairs of HRT 60s and HMI 720s datasets, while the second column does the same for 38 pairs of HRT 60s and HMI 90s datasets. The log density of the pixels is given by the colour scale and is saturated for clarity. The averaged linear fit and y = x are given by the solid grey and dashed black lines, respectively. Panels (a) and (b): Magnetic field strength. Panels (c) and (d): Magnetic field inclination (relative to the LoS). Panels (e) and (f): Magnetic field azimuth. Pixels where $|\varphi^{HMI} - \varphi^{HRT}| > 90$ ° and $|B|^{HRT} < 600$ G are omitted and not included in the fit.

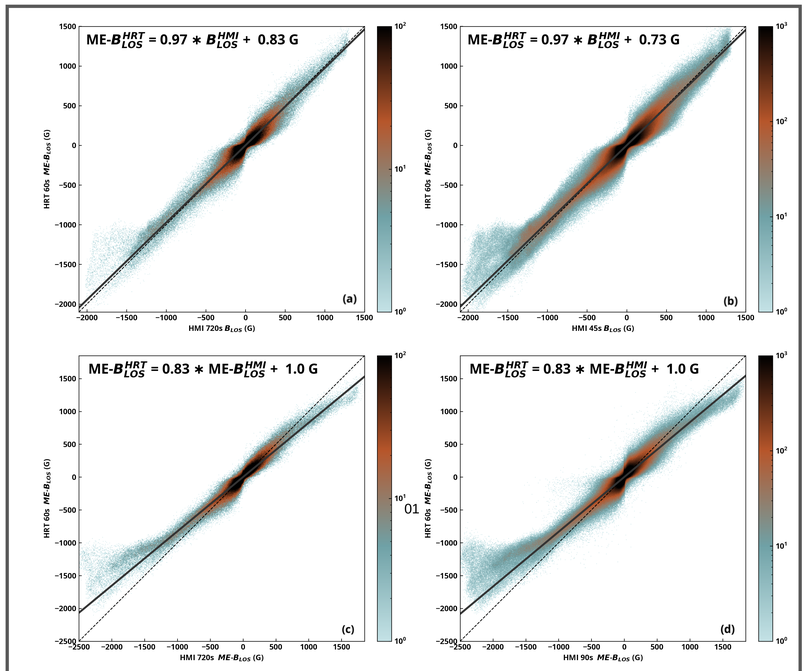

Fig. 4. Scatter plot comparing pairs of SO/PHI-HRT 60s ME-B_{LOS} and HMI B_{LOS} (first row) and HMI ME-B_{LOS} (second row). The log density of the pixels is shown and saturated at 100 (a) and 1000 (b) pixels per plotted point for clarity. The averaged linear fit is shown with the solid grey line, and y = x is indicated by the dashed black line. Panel (a): 7 pairs with HMI 720s B_{LOS}. Panel (b): 56 pairs with HMI 45s B_{LOS}. Panel (c) 7 pairs with HMI 720s ME-B_{LOS}. Panel (d) 38 pairs with HMI 90s ME-B_{LOS}.

CONCLUSIONS

- HRT ME-B_{LOS} very similar to HMI B_{LOS}
- HRT **B** closer to HMI **B** 90s than HMI 720s
- In weak-field regime, HRT measures stronger but more horizontal fields (difference in noise)
- In strong-field regime, HRT measures lower |B| but similar inclination and azimuth
- Due to the observed difference in **B**, the ME-B_{LOS} of the two instruments depart in the strong-field regime

References

[1] Solanki, Sami K., et al. Astronomy & Astrophysics 642 (2020): A11.
[2] Scherrer, Philip Hanby, et al. Solar Physics 275 (2012): 207-227.
[3] DeForest, C. E. Solar Physics 219 (2004): 3-23.
[4] Sinjan, J., et al. arXiv preprint arXiv:2303.16771 (2023). Acceoted by Astronomy & Astrophysics.

Vote Here!

Contact author: sinjan@mps.mpg.de.

Publication PDF